

# Spatial distribution of strains, boron content, and surface potential near dislocation etch pits in HPHT-diamond

Nikolenko A.S.<sup>1</sup>, Danylenko I.M.<sup>1</sup>, Strelchuk V.V.<sup>1</sup>, Lytvyn P.M.<sup>1</sup>, Malyyuta S.V.<sup>1</sup>, Kovalenko T.V.<sup>2</sup>, Suprun O.M.<sup>2</sup>, Lysakovskiy V.V.<sup>2</sup>, Ivakhnenko S.O.<sup>2</sup>

<sup>1</sup> V.E. Lashkaryov Institute of Semiconductor Physics NASU, pr. Nauky 41, 03028 Kyiv, Ukraine

E-mail: Nikolenko.Andrii@gmail.com

<sup>2</sup> V. Bakul Institute for Superhard Materials NASU, Avtozavodska str. 2, 04074 Kyiv, Ukraine

## Introduction

Due to several unique physical properties, boron-doped diamond (BDD) is a promising material for high-power and high-frequency electronics. However, defects and their non-uniform distribution significantly affect the capabilities and properties of diamond-based devices. Using a novel approach of correlative micro-Raman and frequency-modulated Kelvin probe force microscopy (KPFM) mapping, this report studies nano-morphology, local structural, and electrical properties of dislocation etch pits (EPs) in BDD, grown under high pressure and high-temperature conditions (HPHT). This allowed precise measurements of non-uniform distributions of crystallinity, internal strains, boron doping levels, and local surface potential near the dislocation EPs developed during the early stages of selective etching. In addition, micro-Raman mapping revealed a distinct dislocation-induced distribution of boron content and elastic strains with boron-rich and low-boron doped regions and with compressive and tensile stress regions.

## Methods

BDD crystals of cubo-octahedral habit were grown by the temperature gradient method under HPHT conditions in the Fe-Al-B-C system. Atomic force microscopy (AFM), KPFM, and scanning spreading resistance microscopy (SSRM) were used for the characterization of the BDD crystals and multisectoral plates using the NanoScope IIIa Dimension 3000™ scanning probe microscope. Micro-FTIR mapping was performed using the Nicolet Continuum IR microscope coupled to the Nicolet 6700 Fourier spectrometer. Confocal micro-Raman imaging was performed using the Horiba Jobin-Yvon T-64000 spectrometer equipped with the Olympus BX41 microscope and motorized XYZ scanning stage.

## Results

Micro-FTIR spectroscopy was used to estimate the spatial distribution of uncompensated boron impurity  $[N_a - N_d]$  in BDD plates (Fig. 1b) through the analysis of boron-related absorption peaks [1].

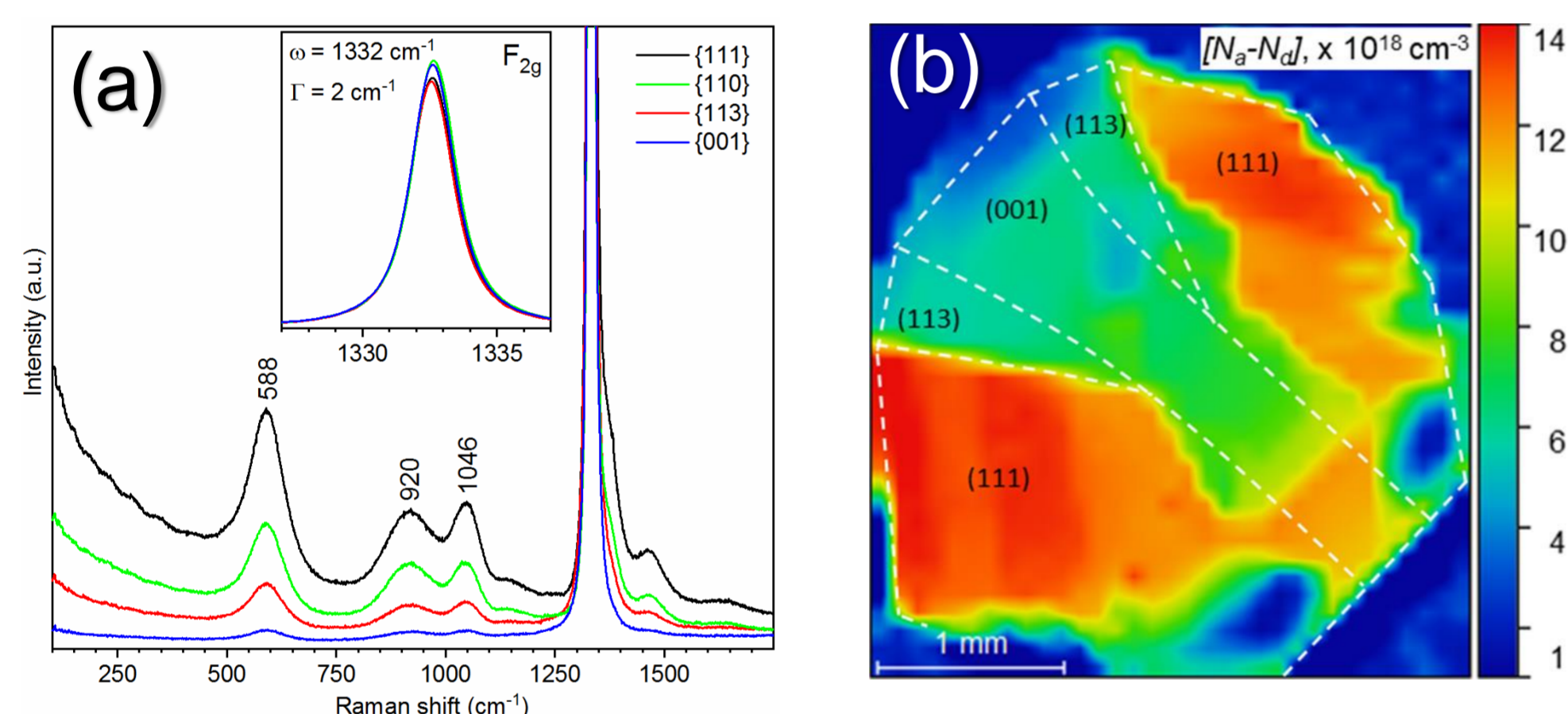


**Fig.1.** Growth-sector dependent Raman spectra of HPHT BDD (a), FTIR map of uncompensated boron impurity  $[N_a - N_d]$  in HPHT diamond plate cut parallel to the growth axis (b). Configuration of the {111}, {113}, and {001} growth sectors is shown schematically by the dashed lines.

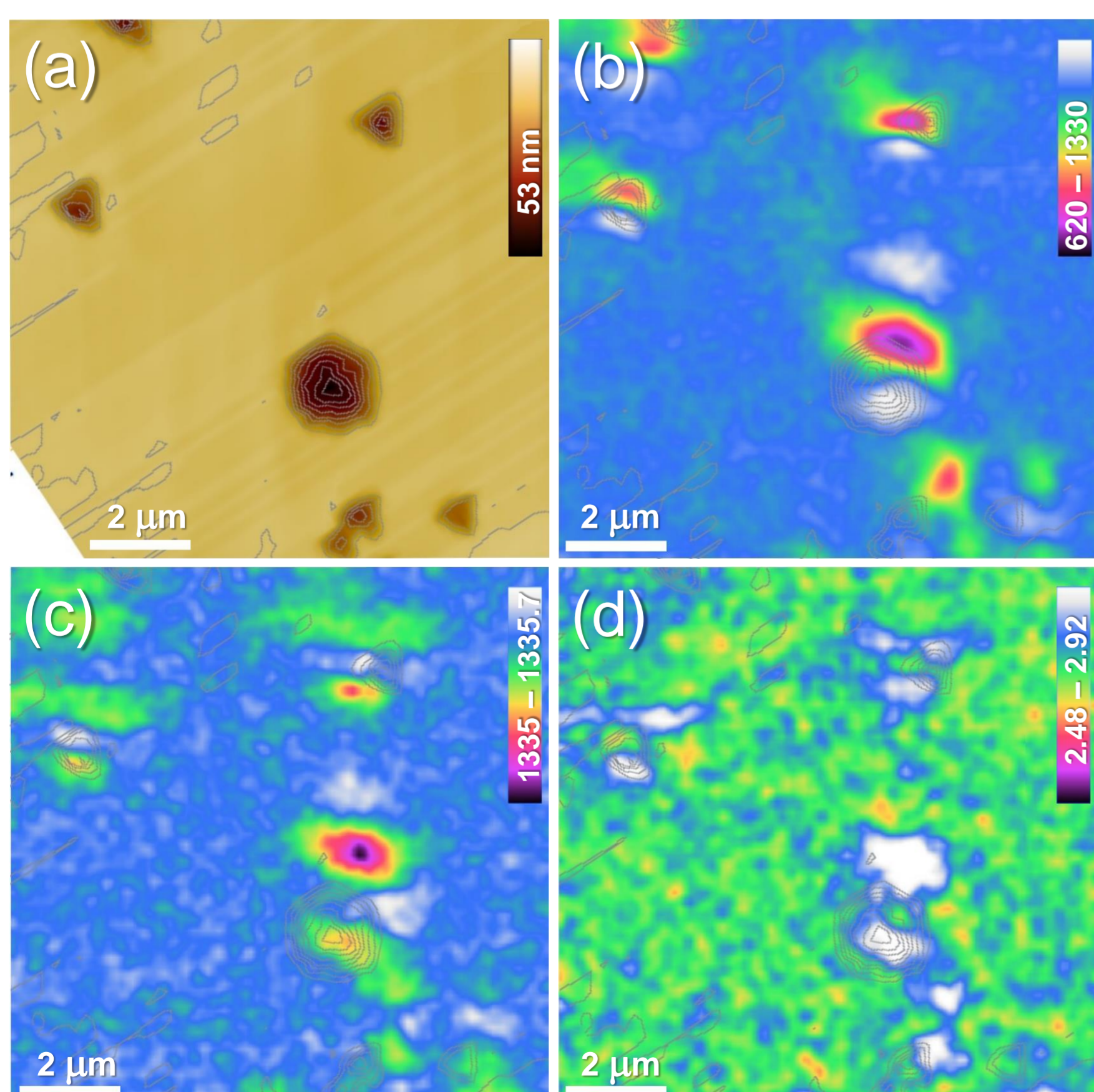


**Fig.2.** AFM height map near the etch pits (a), typical Raman maps of intensity (b), frequency position (c) and FWHM (d) of diamond  $F_{2g}$  peak at  $1330 \text{ cm}^{-1}$  near the etch pits on the growth face of BDD crystal.

Micro-Raman mapping (Fig. 2b-d) revealed non-uniform distribution of intensity, frequency and full-width of diamond  $F_{2g}$  peak near the dislocation EPs, which is caused by variation in crystal quality, strains and boron content. In particular, a distinct dislocation-induced distribution of elastic strains with compressive and tensile stress regions were revealed (Fig. 2c). Analysis of relative intensity of boron-induced Raman peak at  $\sim 580 \text{ cm}^{-1}$  (Fig.3b) demonstrated clear non-uniform distribution of boron content near the EPs with boron-rich and low-boron doped regions.

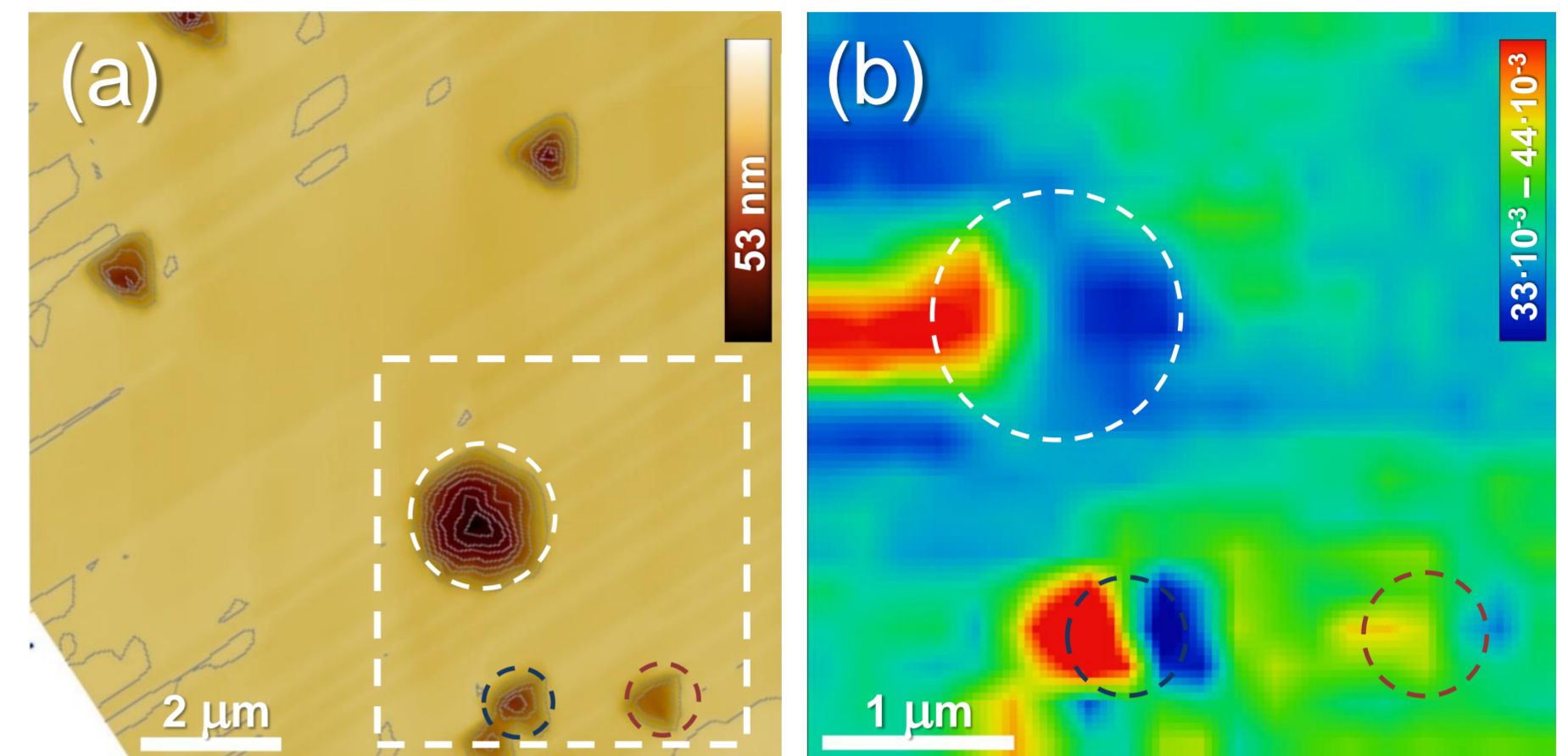


**Fig.3.** (a) AFM height map near the EPs, (b) Raman map of the relative intensity of the boron-induced Raman peak at  $580 \text{ cm}^{-1}$  relative to the diamond  $F_{2g}$  peak at  $1330 \text{ cm}^{-1}$  (the scanned area is marked by dashed rectangle on (a)).

The KPFM analysis demonstrated significant surface potential localization at the EPs and certain terraces. Dislocation EPs on the {111} pristine facet of single-crystal BDD demonstrated a pronounced increase in surface potential (Fig. 4d). This indicates a higher boron content around the dislocation core at the emergent point of dislocation. At the same time, the hexagonal pins are more effectively boron impurity decorated [2]. Note that KPFM is a direct method for measuring local surface potential by mapping the contact potential difference CPD between the metalized microscope probe and the surface:

$$CPD(V) = (\phi_{tip} - \phi_{BDD}) / -e,$$

where  $\phi_{BDD}$  is the work function of BDD crystal, work function of the PtIr probe  $\phi_{tip} = 4.8 \text{ eV}$ . The value of  $\phi_{BDD}$  depends on the electronic affinity  $\chi$ , bandgap width  $E_g$ , the Fermi energy  $E_F$ , the maximum of the valence band  $E_V$ , and the magnitude of the band bending  $\Delta\phi$ :

$$\phi_{BDD} = E_V + E_g - E_F + \chi - \Delta\phi.$$

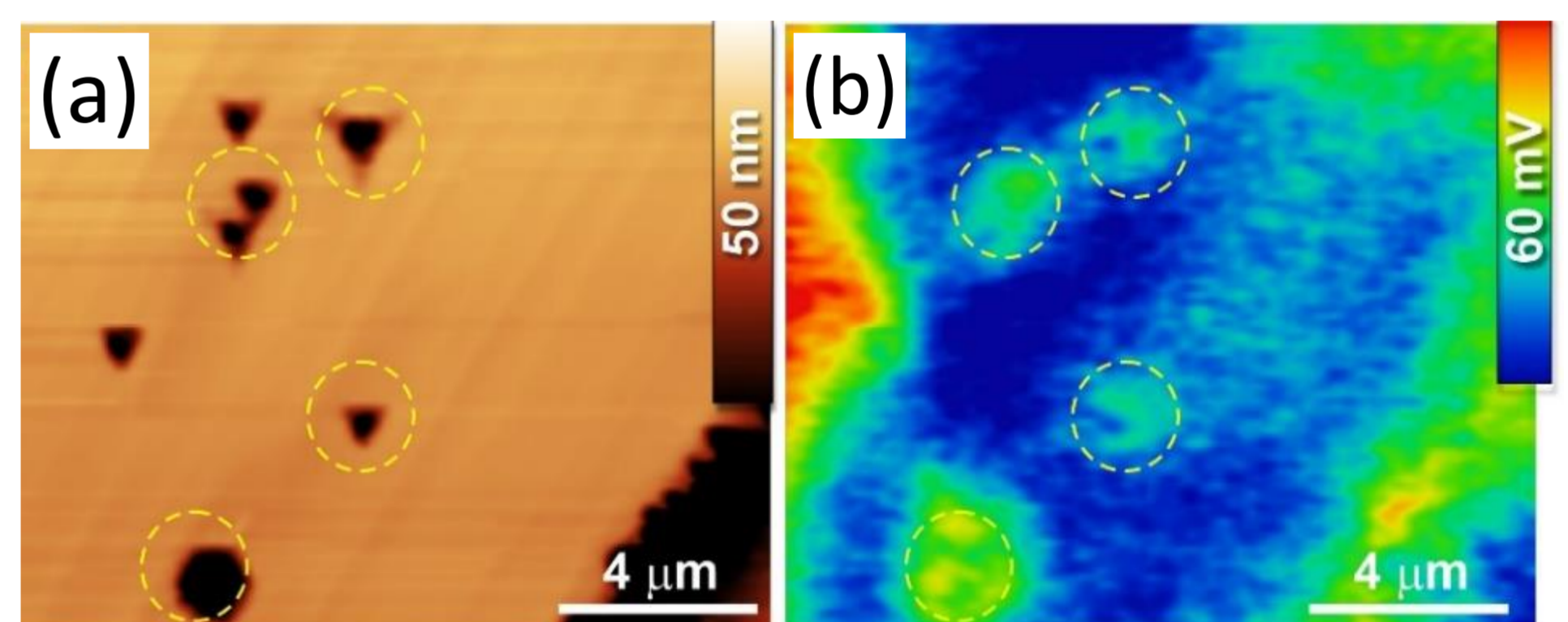


**Fig.4.** KPFM surface potential maps of the etch pits on {111} growth facet of BDD crystal (b). Corresponding height map is shown in (a).

## Conclusions

Spatial distributions of crystallinity, internal strains, boron content, and local surface potential near the dislocation etch pits developed during the early stages of selective etching in boron-doped HPHT-diamond was studied. Micro-Raman mapping revealed a distinct dislocation-induced non-uniform distribution of elastic strains with compressive and tensile stress regions. The spatial distribution of boron content in individual dislocation etch pit was found to be strongly non-uniform with boron-rich regions surrounded by areas with lower boron doping. This is in good correlation with the results of Kelvin probe force microscopy demonstrated a pronounced increase in surface potential near the dislocation etch pits, related to higher boron content around the dislocation core at the emergent point of dislocation. The hexagonal pins were shown to be more effectively boron impurity decorated.

## References

1. D. Howell, et al., Automated FTIR mapping of boron distribution in diamond, *Diam. Relat. Mater.* 96 (2019).
2. A.S. Nikolenko, et al., Correlated Kelvin-probe force microscopy, micro-FTIR and micro-Raman analysis of doping anisotropy in multisectoral boron-doped HPHT diamonds, *Diam. Relat. Mater.* 124 (2022).

## Acknowledgements

The authors are grateful to the National Research Foundation of Ukraine for financial support in the framework of the project № 2020.02/0160 "Development of new carbon solvents compositions for diamond single crystals growth in the thermodynamic stability area with a controlled content of nitrogen and boron impurities in order to create conceptual electronic devices construction".